

Dynamic optical deformations of a chopping secondary mirror

Daniel Vukobratovich,* Robert DiTolla,* and Ralph M. Richard**

***Optical Sciences Center
**Civil Engineering, Engineering Mechanics, and Optical Sciences Center
University of Arizona, Tucson, Arizona 85721**

Abstract

The finite element method was used to analyze the optical performance of the Space Infrared Telescope Facility (SIRTF) fused-silica secondary mirror as it is subjected to a dynamic chopping motion.

The chopping motion was assumed to be of quasi-square wave form with the mirror stationary during a dwell period following the actual chop rotation. The primary optical deformation was "ringing" during the dwell period; damping during the dwell time (20 ms) was not effective. For a given chopping motion, the magnitude of the optical deflections could be reduced by proper choice of the support points, by increasing the stiffness of the mirror, reducing the magnitude of the chop angle, and/or increasing the chop period. Prescribed acceleration versus time during the chop motion affects the optical deformations as well. There are optimum support-point locations for each type of motion.

Tapering the back of the secondary mirror does not significantly affect optical deformation provided that supports are located at the optimum points. For the best trade of mass moment of inertia against deformation, lightweight mirror geometries should be used.

Introduction

The Space Infrared Telescope Facility (SIRTF) is planned as a 1-m-aperture Ritchey-Chretien infrared earth orbital telescope. Diffraction-limited resolution at 2 μm is the performance goal. The IR signal is spatially chopped by oscillating the secondary mirror. To suppress telescope background radiation, the optics will be cooled to 10 K.

The error budget required to meet the resolution goal allots 0.03 μm RMS to the secondary mirror for optical surface deformations created by the chopping motion. To reduce thermal emission by the secondary chopping mechanism, power consumption for the secondary actuators should be minimized. To reduce pointing errors during chopping, the secondary and its associated chopping mechanism should be reactionless.

Although chopping secondary mirrors have been used in balloon-borne infrared telescopes, the performance goal of the SIRTF program requires an advance in the state of current technology. No analytical closed-form solution exists for the dynamic deformations of a chopping mirror.¹ Lack of means of parametrically evaluating the performance of chopping secondaries led to the research, sponsored by the NASA Ames Research Center, which is presented in this paper.

Chopping motion

The chopping motion specified for the SIRTF secondary mirror is in the form of a quasi-square wave. This mirror surface is rotated about a point through an angle θ_{max} in a time t_r , held in this rotated position for a dwell or observation time of t_d , and then returned to the original position (as shown in Figs. 1 and 2). The parameter D, called the duty cycle, characterizes the amount of time available for observation during this operating cycle and is defined as follows:

$$D = 1 - \frac{t_r}{t_r + t_d} \quad (1)$$

As D approaches the optimal value of unity, the time available to rotate the secondary mirror, t_r , becomes small relative to the dwell time, t_d .

Specification of the chopping motion also requires that the chop frequency F be specified. Additionally, the type of path, or time history of the angle of the secondary during the transition time t_r , must be specified.

For this type of chopping motion, the average power P_{AV} required by the secondary mirror actuators, assuming perfect (no loss) actuators, is given by:

$$P_{\text{AV}} = K^2 I F^3 \left(\frac{\theta_{\text{max}}}{1-D} \right)^2 \quad (2)$$

where

K = a path constant
I = the mass moment of inertia of the secondary and mechanism.

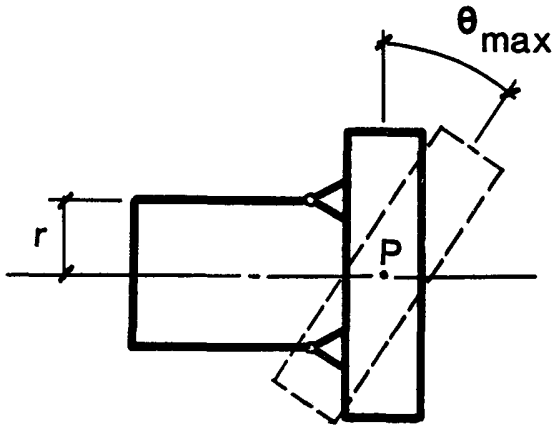


Fig. 1. Chopping motion of the SIRT secondary mirror.

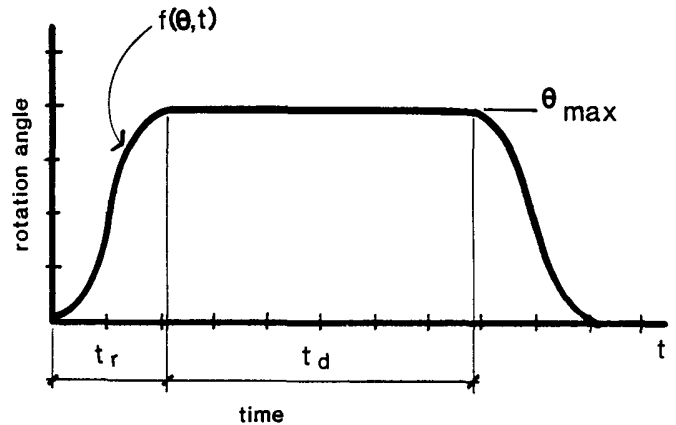


Fig. 2. Input function to a chopping mirror.

Normally, the chop angle, duty cycle, and frequency will be specified. This leaves the mass moment of inertia and path constant as modifiable factors to reduce power. As the pivot point is moved from the center of gravity of the secondary mirror, the moment of inertia is increased by a factor equal to the mass of the secondary mirror multiplied by the square of the distance between the center of gravity and the pivot point. Thus, for a minimum P_{AV} , the secondary should rotate about its center of gravity and have the lowest mass moment of inertia consistent with sufficient mirror stiffness to meet the dynamic optical deformation error budget.

Reactionless operation of the chopping mechanism requires that the instantaneous sum of the shaking forces and shaking moments be zero. This implies that the center of gravity of the mechanism must remain stationary during the chop. The minimum mass moment of inertia for a reactionless system will then be for a pivot about the center of gravity of the secondary mirror.

The path constant can also be changed to reduce power. This changes as the shape of the acceleration curve changes and can vary from 1.5 for a third-order polynomial path to 2.00 for a constant acceleration path. Fortunately, the path constant for simple harmonic motion, which is easy to analyze and control, is 1.57, which is relatively close to the minimum. For this study, a simple harmonic path was chosen.

Although chopping mirrors have traditionally used the optical surface vertex as a pivot point, the difference in optical quality for center of gravity and vertex chopping is very small for most designs.² Center of gravity chopping motion was assumed in this study.

Modeling surface deformation

In the absence of closed-form solutions for dynamic deflections of the secondary mirror during chopping, the finite element method was used. Modifications of the finite element model allow exploration of parametric effects such as the mirror stiffness and support conditions on the dynamic behavior of the mirror.

The finite element model support comprised four equispaced points located on a common radius, r , from the mirror optical axis. Two of the points on a common diameter were fixed points whereas equal and opposite forces were applied at the other two points for the chopping motion.

As a result of this chopping input, each point on the surface of the mirror will undergo a vibratory dynamic response as illustrated in Fig. 3. This vibration is the undamped free vibration response of the mirror to the chopping motion. Deflection of a point on the surface at time t is then described by:³

$$V(t) = e[\delta \cos(\omega t - \phi)] \quad (3)$$

where

e = the dynamic magnification factor caused by the short duration of the loading; it is determined by a relationship between the natural frequency of the structure and the frequency of the input function

δ = maximum displacement from the undeformed surface

ω = the undamped natural circular frequency of the structure

ϕ = phase angle or the angular distance by which the response lags behind the cosine term.

An overall dynamic response of the mirror can be determined by calculating the value of e for each point on the optical surface during the loading interval. These maximum displacements are a function of several important parameters of the mirror design as will be shown later in this paper.

The use of an undamped structural model is justified because of the very low damping coefficient of the candidate secondary mirror materials. Fused silica, one candidate material, has a loss coefficient below 0.001 at 4 K.⁴ For a typical dwell time of 20 ms, this low loss coefficient results in negligible damping effects during the observation period. For beryllium, another candidate secondary mirror material, the loss coefficient at normal "optical" stress levels (below the microyield stress) is 0.015 at 300 K. Again, for small vibration amplitudes, damping effects will be negligible.

In the MSC/NASTRAN finite element program, the "Modal Transient Analysis Method" (Solution 31) provides a dynamic analysis procedure for a structure subjected to enforced motion at its support points. This method first calculates the eigenvalues (frequencies) and associated eigenvectors (mode shapes in model coordinates) for the free vibration response of a discretized model of the structure. A large mass is then assigned to each degree of freedom of the model that is to undergo an enforced displacement. A force numerically equal to that mass multiplied by the defined acceleration at a given time interval (determined from the successive derivatives of the specified chopping input displacement function) is applied to the degrees of freedom that are driven throughout the loading interval.⁵

Quadrilateral and triangular flat-plate bending elements that have membrane, bending, and shear stiffness were used to model the secondary mirror. Alternatively, 8 to 20 node hexahedrons on several layers could have been used. For the enforced chopping motion, a simple harmonic function was used:

$$\theta = \frac{\theta_{\max}}{2} \left[1 - \cos \left(\frac{\pi t}{t_r} \right) \right]. \quad (4)$$

A typical response as calculated by this method to the enforced chopping motion is shown by the contoured detection plot in Fig. 4. To quantify the intensity of deformation, a root-mean-square (rms) of the transverse deflections of the node points from the tilted surface was calculated.

Geometric and stiffness parameters

To develop a better understanding of the dynamic behavior of the secondary mirror, finite element models having various geometries and stiffnesses were analyzed. These studies included the radial location of the support points. This can be illustrated by an analogy to a simply supported beam with a uniformly distributed static load, which is similar to the deflection along a diameter of a plate caused by the inertia forces developed by a chopping input. As shown in Fig. 5, the magnitude of tip deflection of the beam varies as a function of the distance between supports. The tip deflection is zero for support locations at 0.48 L and at 1.0 L. Tip deflection alone does not provide a good measure of the overall deformation of the beam. A better

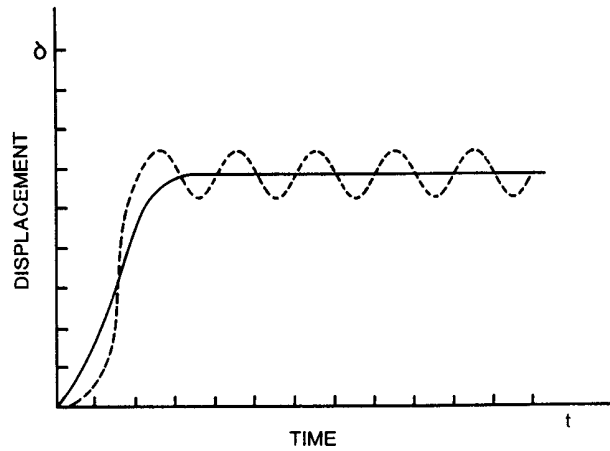


Fig. 3. Vibration response of a point on the optical surface caused by a dynamic chopping motion (actual displacements are exaggerated for clarity).

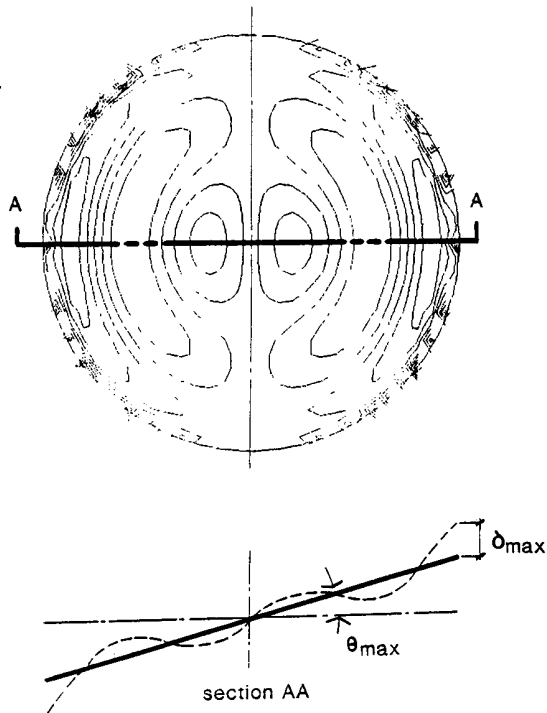


Fig. 4. A typical plot of the deflection contours of a candidate SIRT secondary mirror undergoing a dynamic chopping motion.

measure is the rms of the transverse deflections of all points along the beam. Thus for minimum rms deflection, the optimum support is at 0.48 L. By analogy, the optimum support radius of a secondary mirror, for a diameter of 107 mm is between 0.60 and 0.70 of the diameter. By comparison, for the static mounting of mirrors, the optimum location of a three-support-point system for minimum deflection is at 0.7 of the diameter of the mirror.

Since the deflection of a thin mirror to a chopping motion is flat-plate bending, it is also similar to the beam and plate analogies described above. If the ratio of the applied frequency of the input motion to the fundamental frequency of the mirror is small, of the order of 0.05 to 0.1, the response will be quasi-static produced by the inertia forces that are developed as the mirror is rotated through the chop angle.

For the geometric parameter studies, a circular mirror of constant thickness with a 107 mm diameter was studied. Three mirrors of fused silica and various thickness were modeled. The same loading conditions were used for all models. As shown by Fig. 6, the surface deflections of these mirrors were strongly dependent on the location of the support points. For each mirror thickness there is an optimum radius for the support locations. This radius is at approximately 0.7 of the full radius of the mirror. The 0.03 μm rms tolerance goal of the SIRTf secondary mirror can easily be met for any of the mirrors studied if a proper choice of support radius is made.

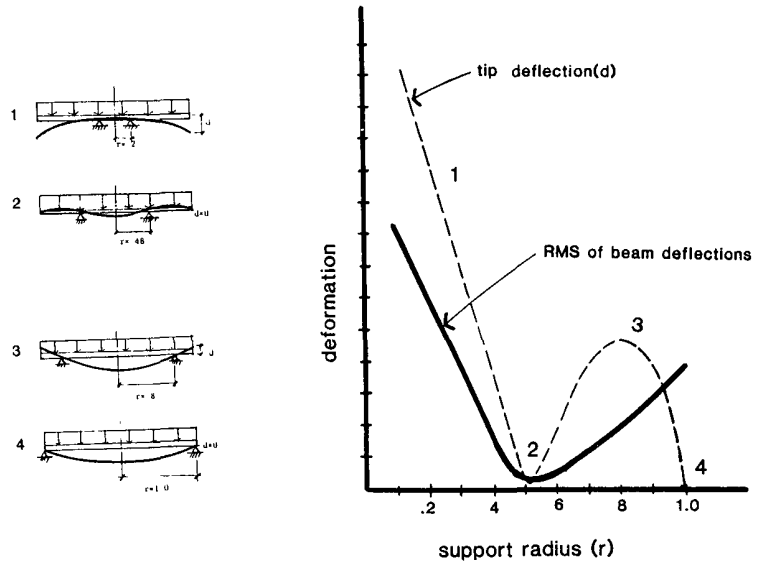


Fig. 5. Static beam analogy for dynamic excitation of a candidate SIRTf secondary mirror.

Since the response of these mirrors to dynamic loading is one of flat-plate bending, deformations can be reduced by selecting a material with high specific stiffness. The specific stiffness coefficient is obtained by dividing the elastic modulus by the material density. To study the effect of specific stiffness, two 5-mm-thick, 107-mm-diameter mirrors were modeled, one of fused silica and one of beryllium. The response of these mirrors under the same loading conditions is shown in Fig. 7. The beryllium mirror, with a specific stiffness 4.8 times greater than fused silica, has significantly less deformation than the fused silica mirror. Again, there is an optimum choice of support radius for the two mirrors studied.

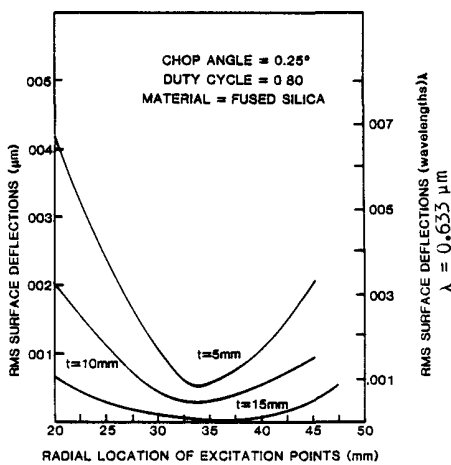


Fig. 6. Surface deflections of a candidate SIRTf secondary mirror for various cross-sectional thicknesses.

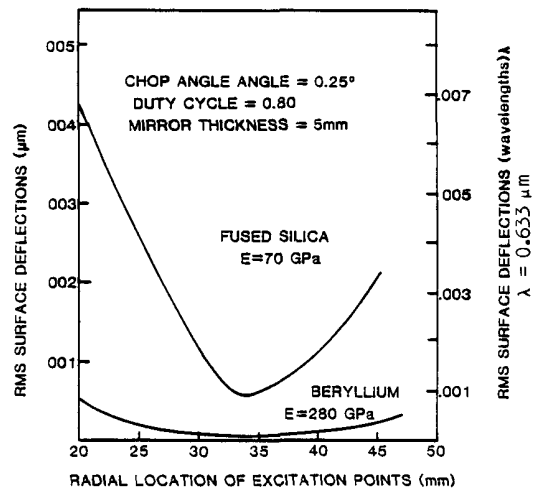


Fig. 7. Surface deflections of the SIRTf secondary mirror for two material stiffnesses.

If the diameter of the mirror is changed, the dynamic deformation of the umirror will scale approximately in accordance with classic thin plate theory. The deflection is proportional to r^4/h^2 . Thus the data presented in the figures can be used for other mirror designs using this scaling factor. For example, an 80-mm-diameter 4-mm-thick fused-silica mirror would have 0.42 times the deflection of the 107-mm-diameter, 5-mm-thick mirror provided that the smaller mirror support locations are scaled linearly.

Tapering the back of the mirror has a relatively small effect on the surface deformation in comparison to the location of the supports. This suggests that tapering the back is a good way to reduce the mass moment of inertia of the mirror without inducing major effects on surface deformations. Lightweight mirror designs that use a honeycomb core generally have the same effect as increasing the material specific stiffness.

Loading parameters

In addition to studying the effect of the mirror geometric and stiffness parameters, the effects of various chopping modes were also considered. The parameters examined were chop angle, duty cycle, and the type of transition path chosen. For all cases, a 107-mm-diameter fused-silica mirror with a 5-mm thickness was modeled.

The magnitude of the surface deflections of the mirror is a linear function of the chop angle for each given transition path because the angular accelerations are proportional to the magnitude of the chop angle.

In this study, only the effects of one cycle of loading have been studied. As stated before, the chopping motion produces an undamped vibration or "ringing" that persists throughout the observation period. Increasing or decreasing the time interval for the rotation of the mirror will change the amplitude of the ringing. A longer time interval for rotation will cause smaller amplitude ringing, but at the cost of reduced duty cycle (reduced observation time). The effects of changing the duty cycle and hence the time available for rotation are shown in Fig. 8. Again, varying the location of the support points has a significant effect on the magnitude and modes of deformation of the mirror. By optimum choice of the support locations, the 0.03 μm tolerance of the SIRTf secondary mirror can be met even for a very severe 0.91 duty cycle.

The type of path or acceleration versus time history of the mirror rotation will also influence the deflection of the mirror. Paths with lower peak accelerations will have lower deflections. This effect is similar to the cam design problem, where peak acceleration can be controlled by the choice of cam profile. Path type has a relatively weak effect on the mirror deflection; the simple harmonic path usually selected for chopping motion has a relatively low acceleration and is suggested as a first design choice. More complex polynomial paths can offer reduced deflection, but have the drawbacks of increased average power and greater control complexity.

Conclusions

The fundamental frequencies of 107-mm-diameter secondary mirrors were calculated to be in the range of 2200 Hz (5-mm-thick fused silica). Frequencies of the applied loading vary between 100 Hz (duty cycle = 0.5) to 400 Hz (duty cycle = 0.91). Because of these large differences in frequencies, these mirrors respond quasi-statically to the inertia forces that are developed during the chopping motion.

The rms deflection varies with material stiffness and the mirror geometric and support parameters. Increasing the specific stiffness (ratio of elastic modulus to the density) of the mirror decreases the deflections in direct proportion. An optimal location of the support points reduces surface deformations significantly. These support points are at 0.7 of the radius of the circular mirror. Deflections scale in accordance with plate theory in the r^4/h^2 ratio.

Changing the loading parameters such as chop angle and duty cycle also affects the surface deformation. Surface deflection scales linearly with chop angle. Increased duty cycle will increase the magnitude of the surface deflection.

Based on these analysis, the 0.03 μm tolerance for dynamic deformation of the secondary mirror for SIRTf can be met in a realistic secondary mirror design.

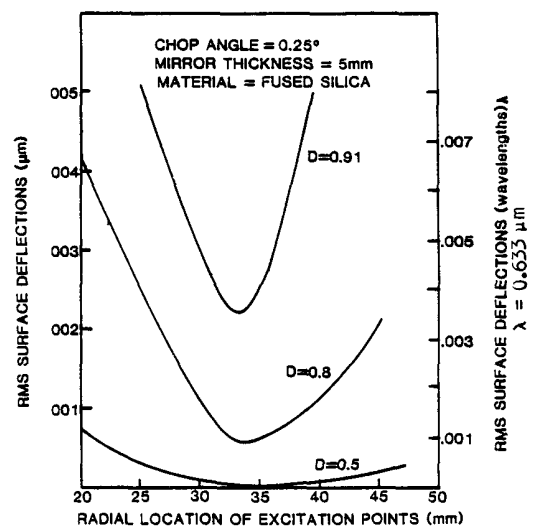


Fig. 8. Surface deflections of the SIRTf secondary mirror for various duty cycles.

References

1. Brosens, P. J., "Dynamic Mirror Distortions in Optical Scanning," Appl. Opt. Vol. 11, p. 2987. 1976.
2. Bottema, M., "Impact of Chopping on Image Quality in the SIRTf Telescope," Proc. SPIE, Vol. 509. 1984.
3. Clough, R. W. and J. Penzien, Dynamics of Structure, McGraw-Hill, New York, 1975.
4. Lee, L. T., A Graphical Compilation of Damping Properties of Both Metallic and Non-Metallic Materials, AFML-TR-66-169. 1966.
5. MacNeal-Schwindler Co., MSC/NASTRAN Application Manual, 1985.